Journal of Computers Vol. 35 No. 5, October 2024, pp. 221-236
doi: 10.53106/199115992024103505015

Research on the Design and Application of a Rapid Inspection System and Method for Ship Curved Plate Forming Based on Binocular Vision

Zhi-Fei Guo[1,2] and Feng Yang[1*]

[1] Department of Mechanical Engineering, Hebei Institute of Mechanical and Electrical Technology, Xingtai City 054000, Hebei Province, China

{guozhifei6669, yangfeng5978}@163.com

[2] Xingtai Technology Innovation Centre for Intelligent Integration and Diagnosis of Metalworking Equipment, Xingtai City 054000, Hebei Province, China

Received 19 July 2024; Revised 29 July 2024; Accepted 15 August 2024

Abstract. Based on the analysis of the actual processing environment, this paper first builds a fast detection system based on binocular vision for the detection of the machining accuracy of ship curved plates. The visual sensors and lenses in the system are analyzed and selected. After selection, the binocular vision is calibrated using Zhengyou Zhang's calibration method, and visual distortion is corrected through matrix transformation. Then, in order to complete the calculation of the curvature of the ship's curved board, a curvature calculation model for the ship's curved board was constructed. The model can calculate the curvature information and depth information of the curved board, and then solve the curvature information and depth information models separately using the least squares method. Finally, to verify the accuracy of the visual system, a simulation experimental platform based on software and hardware was built. After simulation experiments, the curvature error probability and measurement time of the curved board were obtained, and the results met expectations.

Keywords: ship curved board, binocular vision, least square method

1 Introduction

In recent years, due to the increase in transportation, military and maritime activities, China's shipbuilding industry has developed rapidly, ranking among the top in the international market share. Currently, it has become one of the world's most important shipbuilding bases and has also developed multiple shipyards with global status. According to the latest data released by the China Shipbuilding Industry Association, the international market share of China's three major shipbuilding indicators, in terms of deadweight tonnage and corrected total tonnage, remains world leading. Although China is a world leader in shipbuilding scale, there is still a significant gap between China and traditional shipbuilding powers in shipbuilding technology and ship manufacturing inspection technology. Therefore, strengthening the research and development of green products, eliminating and improving outdated production and manufacturing inspection processes, enhancing the core competitiveness of shipbuilding enterprises, and promoting high-quality development strategies are the development goals of China's shipbuilding industry [1].

The manufacturing of large ship hulls is carried out by welding a large number of curved steel plates of different styles according to the construction process of the hull. The outer plate of the hull is a large complex free-form surface with a certain curvature. Due to the numerous types and tonnages of ships, as well as the complexity of the hull profile compared to a single hull, there are complex rib lines, height/horizontal inspection lines, longitudinal and transverse joint lines, etc. These lines determine the degree of ship formation. Due to the large thickness and high strength of ship curved plates, there are many factors that affect the local deformation of the plates during the processing. It is difficult to process the curved plates in one go and generally requires multiple processing and measurements, which is a multi-step asymptotic process. In the process of forming ship curved plates, it is particularly important to monitor the forming status of curved plates in order to accurately determine whether the forming meets the processing requirements and to correct the processing parameters for the next step. The main detection object of this article is the ship's single curvature board, as it is mainly used in ships [2].

Traditional ship curvature detection relies on manual labor, using tools such as triangular templates and flexi-

* Corresponding Author

ble templates, which are labor-intensive and cumbersome to operate. More importantly, traditional manual measurement methods have low measurement efficiency, poor accuracy, and unquantifiable errors. The development of computer vision technology provides technical support for non-contact and rapid measurement methods. Currently, digital detection methods represented by binocular 3D vision measurement technology have significant advantages such as high detection efficiency, high accuracy, non-contact, and low cost, and have been widely applied in the automation detection industry. Binocular vision is an important function in the human visual system. By observing an object with both eyes simultaneously, we can perceive and understand its three-dimensional shape, size, and depth information. In the field of computer vision, using binocular vision for object size measurement has become a common and effective method. Binocular vision is the use of two cameras to capture object information in the same scene, and then obtain depth information relative to the camera imaging plane in the 3D scene from the captured images based on the principle of triangulation [3].

Therefore, this article focuses on the measurement of single curvature plates on ship curved boards as follows:

1) Based on the actual situation, the processing environment was analyzed, and the design parameters of the visual system were determined accordingly. A binocular vision inspection system was built, and the selection of cameras and lenses was completed;

2) In terms of precision adjustment of the camera, matrix equations were established for the camera, and camera calibration and visual distortion correction were performed through matrix transformation;

3) A curvature and depth information model for ship curved plates was established, and the least squares method was used to solve the curvature and depth information of the curved plates;

4) In order to verify the rationality of the visual system in this article, a simulation experimental environment was built and a complete software system framework was constructed.

2 Related Work

There are many scenarios where binocular vision is applied to size measurement. Zhengjia Wang uses binocular vision to measure the outer contour of vehicles. Firstly, the vehicle images captured by binocular cameras are corrected, and an improved stereo matching algorithm is used to calculate and generate the vehicle disparity map. Based on the principle of binocular vision 3D measurement, calculate the vehicle contour disparity information for 3D reconstruction and generate the vehicle point cloud. Aiming at the problem of missing vehicle contour data in camera blind spots, a point cloud symmetry repair method based on license plate recognition was designed to generate a complete 3D contour of the vehicle. The experimental results show that the measurement indication errors of the three vehicle models are all less than 1% [4].

Jiawei Zhang proposed a pipe diameter measurement method that integrates multiple sets of binocular vision systems. Multiple sets of binocular cameras are used to capture images, reconstruct 3D images, and fuse coordinates of multiple laser markers projected on the pipeline measurement section. The external pipe diameter, ellipticity, and other dimensional parameters are obtained through ellipse fitting. This method achieves automatic matching of feature points through affine distance transformation algorithm, and uses an optimized point cloud registration algorithm with normal vector constraints to ensure the accuracy of coordinate fusion. The experimental results show that the relative error measured by the system is within ± 0.570%, the maximum repeatability standard deviation is 0.551 mm, and the longest measurement time is 1.5 seconds [5].

Xiaoyu Yan from Anhui University designed a stereo vision system based on the principle of binocular measurement, combining OpenCV and Matlab, to achieve distance information between the camera and the target object. The system used BM (Block Matching) stereo matching algorithm to complete stereo correction and matching of the camera in the VS2017 environment and OpenCV 3.4.7 library, thereby obtaining a disparity map; Finally, a binocular camera was used in the experiment, and code was written to obtain the corresponding world coordinates by clicking on the disparity map with the mouse to measure the object distance; The experimental results show that when the distance between the measured object and the camera's optical center is within the range of 500-700 mm, the relative error percentage between the measured distance and the actual distance is between 0.171% and 0.192%, and the experimental error is less than 5% within 2950 mm, which meets the experimental accuracy requirements [6].

In the field of automated detection of ship curved plates, some scholars have also conducted research, but there are relatively few related achievements. Now, representative research results will be summarized and their respective shortcomings will be analyzed.

Liang Zhao proposed a computer binocular vision measurement method based on structured light assisted

scanning for the complex working environment in shipbuilding sites and the large-scale curved plates of ship hulls. Using the Zhengyou Zhang calibration method to calculate the internal and external parameters of the camera, laser lines are initially extracted from the image based on color space and morphological processing. The sub-pixel level laser centerline is obtained using the Steger algorithm based on the Hessian matrix. The laser point coordinates are calculated using the epipolar matching method, and edge points are selected based on the second-order partial derivative. This non-contact measurement method has high accuracy and good applicability, and can meet the requirements of curved plate detection in shipbuilding. However, the article only proposes a detection method and has not formed a rapid detection system [7].

Shunshun Zhao developed an in-situ detection and automatic adjustment system based on line laser multi vision technology suitable for the CNC 3D bending machine processing site, in order to achieve fast and accurate in-situ detection and automatic adjustment of ship curved plates through progressive forming. A detection system scheme and structural parameters were designed, and key technologies such as system calibration, line laser 3D reconstruction, point cloud registration, calculation of ship plate forming deviation and sheet rebound were studied. A software system for in-situ detection and automatic shape adjustment based on the Windows platform was developed. The results show that the measurement error of the system is less than ± 1mm, the single measurement time is less than 30s, and the field of view is larger than the bending machine processing area of 2750mm × 2750mm, which meets the requirements of in-situ detection and automatic shape adjustment of ship plates in the CNC 3D bending machine processing process. However, the entire system takes a long time to measure and cannot meet the requirements for rapid detection [8].

Delin Hu proposed a non-contact computer vision based photogrammetric method for ship hull curvature. The camera calibration algorithm was used to calibrate the internal and external parameters of the camera. To obtain more feature information on the surface of the ship hull curvature, a photogrammetric method was proposed by projecting structured light onto the surface of the ship hull curvature; And based on the AKAZE feature extraction algorithm, the KNN machine learning algorithm is combined with the RANSAC algorithm for feature matching and optimization. The feature-based quasi dense diffusion algorithm is used to achieve high-precision 3D reconstruction of the ship's curved plate. A computer vision based binocular photogrammetry system is built for camera calibration experiments and ship's curved plate measurement experiments, with measurement errors less than 1 mm, meeting the accuracy requirements of shipbuilding. However, the article did not provide a detailed introduction to the construction process of the measurement system, lacking a more effective understanding of its significance [9].

Therefore, this article proposes a design of a rapid retrieval system for the forming accuracy of ship curved plates based on binocular vision, and provides a detailed introduction to the curvature measurement method. The composition of the article is as follows: Chapter 2 is about the research results of relevant scholars, Chapter 3 mainly introduces the construction process of the binocular vision detection system, Chapter 4 is the method and process of measuring the curvature information of ship curved plates, Chapter 5 is the simulation experiment, and Chapter 6 is the conclusion section.

3 Construction of Binocular Vision Detection System

The binocular vision curvature detection system is generally placed in the curved plate processing workshop. The design purpose is to quickly detect the ship's curved plates through a conveyor device immediately after processing. Therefore, in order to design a binocular stereo vision measurement sensor that meets the requirements of ship curved plate forming detection, this section first conducts research and analysis on the ship's curved plate forming process and working conditions.

The processing of curved plates generally adopts forming processes such as cold processing or hot processing to bend flat plates into a curved surface shape consistent with the theoretical CAD model. The commonly used ship bending forming techniques mainly include mechanical cold bending (such as roll bending, compression bending) and wire heating forming (such as water fire bending process). For large-sized single curvature hull outer panels, mechanical cold bending processes such as roll bending are usually used. For small-sized complex hyperbolic hull outer panels, mechanical cold bending method can be used to process the curvature in one direction first, and then the water fire bending process can be used to process the other curved panel.

According to the forming process requirements and complex on-site working conditions of ship curved plates, the following requirements have been put forward for the performance indicators of binocular stereo vision measurement sensors in the production site [10].

1) The size of the curved board is generally larger, so the selection of visual sensors should have a larger field of view and a faster in-situ measurement speed. To improve the efficiency of in-situ forming processing, the single angle measurement time of the measuring sensor should be less than 10 seconds,

2) The working environment of the detection system contains high temperature and dust, so the detection system, especially the visual sensor, should be able to work normally in this environment and have functions such as temperature compensation.

3) Finally, in order to minimize the interference of measurement sensors on workers' water and fire operations, it is recommended that the distance between the sensor and the water and fire operation platform be greater than 2 meters. At the same time, in order to ensure the safe operation of the vehicles above the workshop, the installation position of the measuring sensor should not exceed 3 meters from the water fire operation platform.

The overall detection indicators of the system are shown in Table 1.

Table 1. Overall design requirements for system detection

Check the accuracy	Detection time	Detection range	Work distance
$\leq 2mm$	$\leq 10s$	$\geq 3000 \times 3000mm$	$3000mm$

3.1 Construction of Binocular Vision Measurement System

The entire measurement system consists of computer control module, binocular vision module, communication module, transmission module, and handling module, as well as measurement software module [11]. The composition and functional description of each module are as follows:

1) The computer control module mainly installs detection system software. By installing existing software systems or running self-developed measurement control components, it can display real-time measurement results and serve as the brain of the entire measurement system, with the computer control module as the communication turnover unit.

2) The binocular vision module is mainly composed of binocular cameras. According to design requirements, a depth camera or two monocular cameras can be used to measure curvature through joint calibration of the cameras.

3) The communication module is based on TCP/IP communication protocol to complete communication and data exchange between the upper computer PC and the robotic arm.

4) The conveyor module is mainly composed of a conveyor belt. The starting point of the conveyor belt is the end of the ship's curved board processing. After the processing is completed, the handling module automatically transports the curved board to the conveyor belt, and then the conveying module transports the curved board to the designated position for curvature detection.

5) Measurement software, also known as measurement system, is a module designed specifically for this detection system. The system mainly includes a main interface, display interface, work interface, etc.

The overall framework of the work system is shown in Fig. 1.

3.2 Hardware Selection

In terms of hardware selection, the core components of the measurement system in this article are the camera and lens, so the main focus is on the selection process of the lens and camera.

Camera performance directly affects image quality, and it is particularly important to choose a certain model of camera. As of now, imaging chips in cameras include CCD and CMOS [12]. CCD chip is a semiconductor imaging device that converts optical signals into electrical signals. In practical use, it is widely used due to its small size, low power consumption, high sensitivity, and long usage time. As another type of image sensor, although CMOS chips have lower power consumption and lower prices, due to process technology, the resolution of CCD chips with the same size and volume is much higher than that of CMOS chips. In order to improve the accuracy of measuring large-sized parts, this chapter requires very high specifications for the image quality and resolution parameters captured by the camera. Taking into account other performance factors, this chapter has chosen the MER3-506-58G3M/C-P industrial camera from Daheng Company. The MER3-506-58G3M/C-P uses a CCD chip to transmit image data through its unique GigE data interface, and this model of camera also integrates an I/

O interface. The transmission part of the MER3-G3-P camera is based on 2.5GBASE-T technology, with a maximum transmission rate of 2.5Gbps and support for rate switching to 1Gbps, greatly improving the transmission of network cameras. The 2.5GigE camera maintains a 1GigE camera volume while increasing bandwidth by 2.5 times. Due to the significant increase in transmission speed, the power consumption of the 2.5GigE camera has significantly increased. The MER3-G3-P camera adopts passive heat dissipation technology, which maximizes the transmission capacity of the camera within a limited volume. The camera has high reliability and strong environmental adaptability. The camera parameters are shown in Table 2.

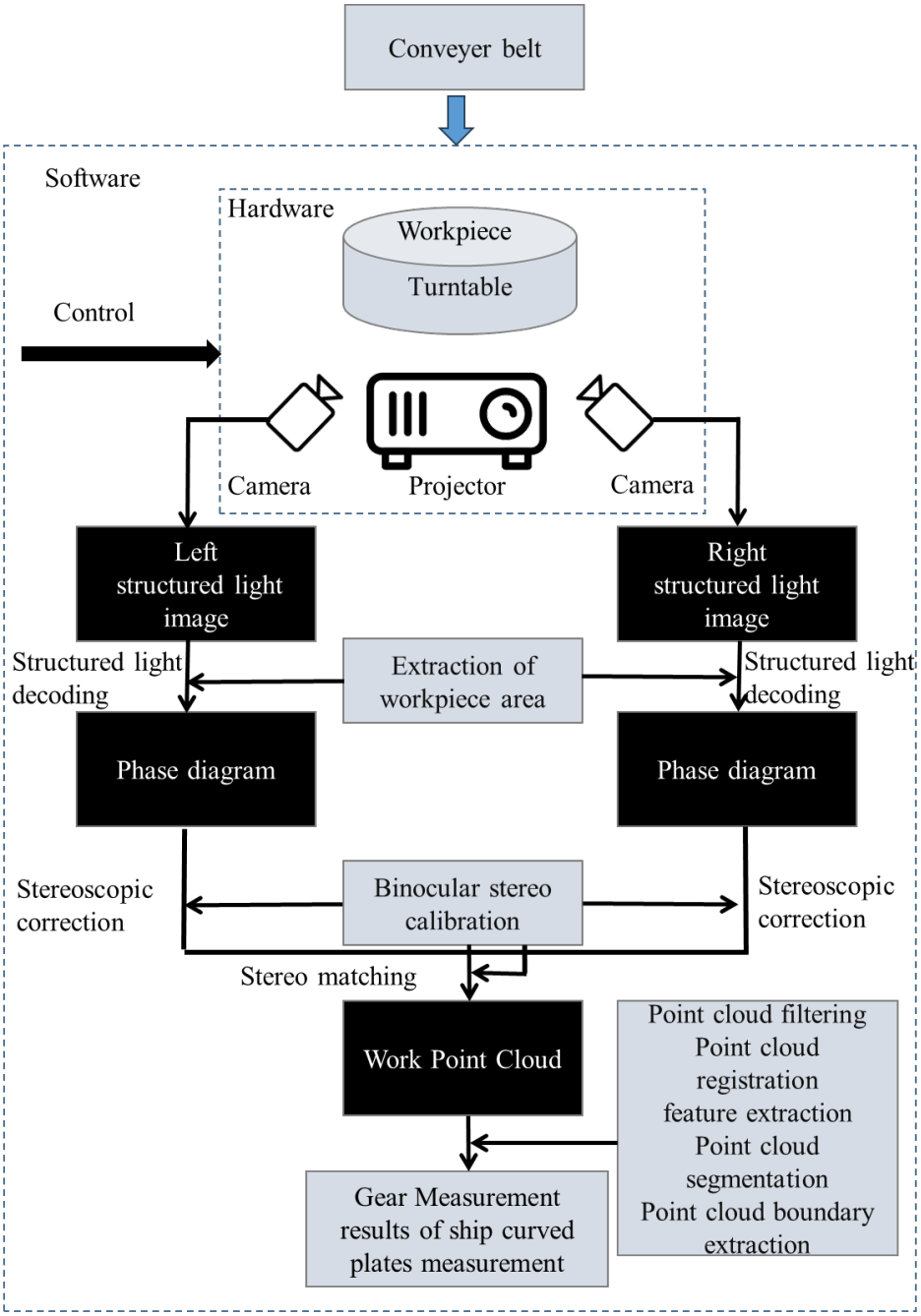

Fig. 1. Overall framework of visual inspection system

Table 2. MER3-506-58G3M/C-P Camera Parameter List

Parameter	Parameter values
Pixel size	$2.74\mu m$
Resolution ratio	2448×2048
Frame rate	58.6fps
Pixel depth	$12bit$
Working voltage	12-24V

The lens selection mainly considers the following issues:

1) The interface between the camera and lens, the Mercury third-generation 2.5GigE digital camera uses the standard C interface. When selecting a lens, choose a lens with the same interface

2) The maximum CCD/CMOS chip size that can be covered by lens imaging. There are mainly 1/2 “, 2/3”, 1/1.2 “, 1”, 1.1 “, 4/3”, etc. When selecting lenses, it is necessary to ensure that the lens target surface is not smaller than the target surface (CCD/CMOS chip) size of the digital camera.

3) Focal length is the distance between the center point of the lens and the clear image formed on the focal plane [13]. The smaller the focal length value, the larger the field of view captured by the digital camera. The focal length is calculated using the following formula:

$$f = \frac{d_{CCD/CMOS} * L}{S_{CCD/CMOS}} \tag{1}$$

In the formula, A represents the focal length, B represents the horizontal or vertical dimension, C represents the working distance, and D represents the field of view of the image. After the above calculation, the lens model is selected as HN-5M series, and the lens parameters are shown in Table 3.

Table 3. MER3-506-58G3M/C-P camera parameter list

Parameter	Parameter values
Outside diameter	$29.5mm$
Resolution ratio	5 million pixels
Number of installation holes	3

3.3 Camera Calibration

Considering the high precision required for target measurement, the position of the camera is fixed in actual scenes, and the internal and external parameters of each camera are not exactly the same. Therefore, the first monocular calibration method adopted in this paper is based on the Zhengyou Zhang calibration method based on checkerboard pattern [14], using a two-dimensional plane template, changing the template angle multiple times, capturing multiple images of the same plane template at different angles, and solving the internal and external parameters of the camera.

The Zhengyou Zhang plane calibration method uses a checkerboard lattice as the calibration template. Due to the use of too many points, there are many sources of error in the calibration point detection and matching process. Wen Tao et al. proposed using a calibration algorithm based on a cross grid instead of a checkerboard lattice, which can obtain more accurate position information in strong light and noise situations. However, the design of the template is still quite complicated, and the line width needs to be accurate to 2mm.

The image coordinate system (x_i, y_i) is a coordinate system established based on the two-dimensional image captured by the camera. The intersection point (x_o, y_o) between the camera’s optical axis and the imaging plane is its origin, and its pixel coordinate system is (x_p, y_p). The origin is set at the upper left corner of the two-dimensional image [15]. The conversion relationship between (x_i, y_i) and (x_p, y_p) is as follows:

$$\begin{cases} x_p = \dfrac{x_i}{dx_i} + x_0 \\ y_p = \dfrac{y_i}{dy_i} + y_0 \end{cases} \tag{2}$$

The above values are all related to the camera and are called internal parameters. Write the above equation in matrix form using homogeneous coordinates for subsequent calculations:

$$\begin{bmatrix} x_p \\ y_p \\ 1 \end{bmatrix} = \begin{bmatrix} \dfrac{1}{dx_i} & 0 & x_o \\ 0 & \dfrac{1}{dy_i} & y_0 \\ 0 & 0 & 1 \end{bmatrix} \begin{bmatrix} x_i \\ y_i \\ 1 \end{bmatrix} \tag{3}$$

The transformation relationship between coordinate systems is shown in Fig. 2.

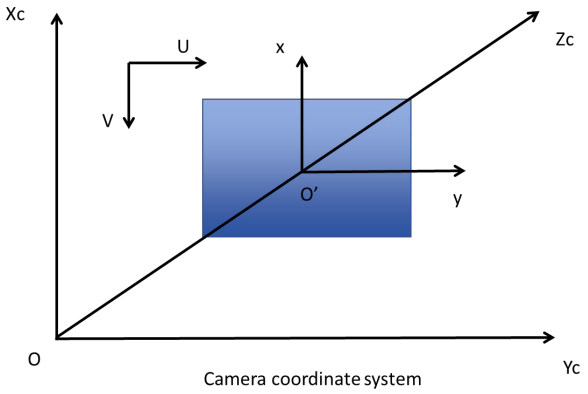

Fig. 2. Coordinate transformation relationship

The world coordinates can be transformed into a camera coordinate system through simple rigid body transformations, such as translation and rotation. The camera coordinate system is represented as (x_c, y_c, z_c), and its mathematical expression is as follows:

$$\begin{cases} x_c = Rx_W + M \\ y_c = Ry_W + M \\ z_c = Rz_W + M \end{cases} \tag{4}$$

In the formula, (x_W, y_W, z_W) is the world coordinate system, R represents the rotation matrix, and M represents the translation vector. Because the values of R and M are independent of the camera, they are called extrinsic parameters. After the camera coordinate system undergoes perspective transformation, the image coordinate system is obtained. The relationship between camera coordinates and image coordinates at point $P(x_P, y_P)$ captured by the camera is expressed as:

$$\begin{cases} x_P = \dfrac{f}{L_A} x_i \\ y_P = \dfrac{f}{L_A} y_i \end{cases} \tag{5}$$

By combining all the above processes, the camera matrix G_c can be obtained, thereby obtaining the geometric model of the camera, namely the camera model.

$$G_c = \begin{bmatrix} G_{11} & G_{12} & G_{13} & G_{14} \\ G_{21} & G_{22} & G_{23} & G_{24} \\ G_{31} & G_{32} & G_{33} & G_{34} \end{bmatrix} \tag{6}$$

Let the camera's internal parameter matrix be represented as:

$$N = \begin{bmatrix} \dfrac{f}{dx_i} & 0 & x_0 \\ 0 & \dfrac{f}{dy_i} & y_0 \\ 0 & 0 & 1 \\ \end{bmatrix} \tag{7}$$

There are two constraints in the camera model [16]:

1) Due to the rotation of coordinates around the X and Y axes, the corresponding elements in the rotation matrix are orthogonal, and their vector product is 0.

2) The modulus of the rotated proof vector is 1.

As can be seen from the previous text, after obtaining several images of a chessboard pattern, the internal parameter matrix N.

Camera admission videos inevitably introduce distortion because there is no perfect lens in real life. Prior to this, the calibration procedures of Zhengyou Zhang did not take into account camera distortion. However, the camera may experience radial distortion due to the shape of the lens, and tangential distortion may occur due to the lack of strict parallelism between the lens and the imaging plane during installation. Among them, radial distortion dominates in distortion, while tangential distortion has a relatively small impact. Due to errors in camera installation and the control of relative lens technology, the controllability at the installation level is easier to control than the lens technology. Therefore, radial distortion dominates camera distortion in distortion. Therefore, this article only considers camera radial distortion for Zhengyou Zhang's calibration method.

Due to the fact that radial distortion is relatively small in practical situations, the first two terms of the Taylor series expansion around the principal point (x_o, y_o) are used to determine the distortion coefficients λ_1 and λ_2 of radial distortion, which are expressed as follows:

$$(\hat{x}, y) = (x, y) + \left[(x, y) - (x_0, y_0)\right]\left[(\lambda_1 + \lambda_2)(x^2 + y^2)\right] \tag{8}$$

(x, y) represents the ideal undistorted pixel coordinates, which can be solved by the camera model through the world coordinate points of the object. $(\hat{x}, y)$ represents the pixel coordinates with radial distortion in actual situations, and the distortion coefficients λ_1 and λ_2 can be calculated.

Use a camera to capture a checkerboard calibration board, and then use the calibrateCamer() function to calibrate all images of the calibration board, obtaining the internal and external parameters of the camera, as shown in Table 4.

Table 4. Calibration results of binocular camera parameters

	Left camera	Right camera
Internal reference matrix	$\begin{bmatrix} 876.78 & -0.68 & 376.06 \\ 0 & 876.89 & 265.28 \\ 0 & 0 & 1 \end{bmatrix}$	$\begin{bmatrix} 819.29 & -1.13 & 367.91 \\ 0 & 827.01 & 272.62 \\ 0 & 0 & 1 \end{bmatrix}$
Distortion matrix	$\begin{bmatrix} -0.399 & 0.282 & -0.002 & 0.005 & -0.063 \end{bmatrix}$	$\begin{bmatrix} -0.401 & 0.207 & -0.005 & 0.003 & -0.047 \end{bmatrix}$
Rotation matrix	$\begin{bmatrix} 1 & -0.006765 & -0.002583 \\ -0.00898 & 1 & -0.008978 \\ 0.001987 & 0.007891 & 1 \end{bmatrix}$	
Translation matrix	$\begin{bmatrix} -65.8672 & -0.08879 & -0.2917 \end{bmatrix}$	

Under the principle of stereo correction in binocular cameras, the undistort function is used to remove distortion from the image, resulting in more accurate image results [17]. The comparison of the images before and after correction can be seen in Fig. 3, and it can be clearly observed that the uncorrected images have significant camera distortion effects.

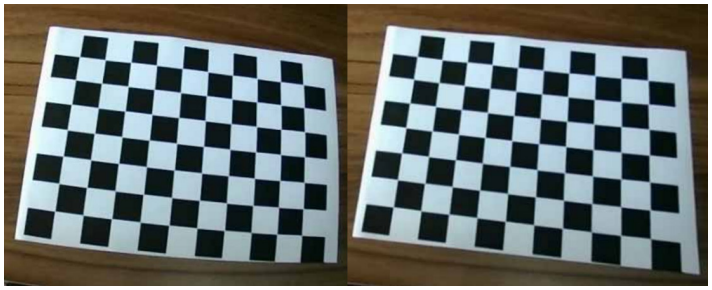

Fig. 3. Camera calibration results

After the above process, this article used the Zhengyou Zhang calibration method to complete the calibration process of the left and right cameras, while considering the principle of camera imaging, and completed the correction of radial distortion of the camera.

4 Measurement Method for Curved Plates of Ships

In the previous chapter, a binocular vision detection system was built to complete the calibration and setting of the visual level. After the visual system completes the image acquisition, it needs to process and recognize the image. To achieve the measurement of ship curvature and the detection of ship curvature by binocular vision, the image is first preprocessed, and then the preprocessed point cloud image is compared and measured. The detection process is shown in Fig. 4.

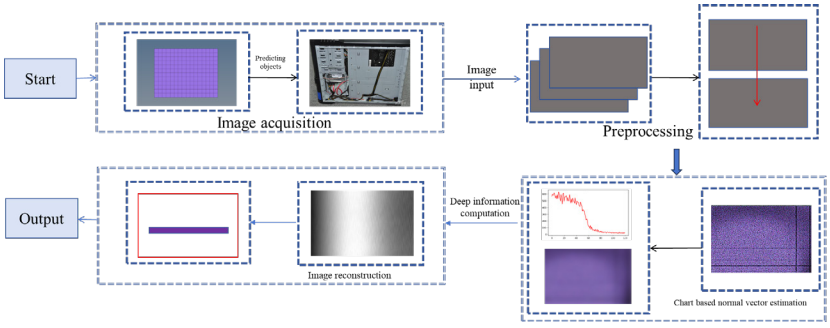

Fig. 4. Ship curved plate inspection process

4.1 Image Preprocessing

After the data collection is completed, due to the surface material of the object, beam splitting, and other reasons, there is weak and inconspicuous noise around the feature point group after splitting. However, the pixel intensity of the image contains the three-dimensional information of the object. In order to avoid interference with the subsequent calculations of the experiment, it is necessary to denoise the image [18]. However, the noise in the image is not obvious and difficult to distinguish with the naked eye. In order to make the feature points in the image more prominent, this paper uses an adaptive thresholding method to denoise the noise in the image. This method calculates the local threshold based on the brightness distribution of different regions of the image, and can adaptively calculate different thresholds for different regions of the image. By using the difference in grayscale values between adjacent image pixels, the noise is removed and the image feature information is highlighted, achieving the separation of useful and useless information and preventing interference from useless information. In the image preprocessing stage, this paper adopts conventional image preprocessing methods, so detailed method introductions are not provided in this paper.

4.2 Calculation of Surface Normal Vectors

To achieve the detection of object curvature, it is necessary to calculate the surface normal vector of the object. The Lambert model assumes that the surface of the object is smooth, and the incident light has the same radiance in all directions after being reflected by a completely diffuse reflector surface. The intensity of diffuse reflection is proportional to the cosine of the incident angle and independent of the reflection direction. The Lambert model assumes that the surface of an object is smooth, however, in reality, many objects have relatively rough surfaces that are uneven at the microscopic level and can be seen as a collection of many micro surfaces. When drawing a relatively rough diffuse reflective material object surface, at high resolution, each pixel in the generated image approximately contains only one micro surface, and the assumption of the Lambert model is still reasonable. However, at low resolution, each pixel in the generated image may contain a large number of micro surfaces, and the assumption of the Lambert model is biased [19].

According to the principle of Lambertian reflection model, it is known that the pixel intensity of each point in an image is related to the product of the surface normal vector of each point of the object and the direction of the light source. The grayscale value of any point in the image is equal to the product of the surface reflectance, surface normal vector, and light source direction vector of that point, written in matrix form as follows:

$$G_{ra} = \eta \cdot N_{vec} \cdot L \tag{9}$$

In the formula, G_{ra} is the grayscale value of the image pixel, η is the reflection coefficient of the object surface, N_{vec} is the normalized normal vector of the object surface, and L is the normalized light source vector.

Need to solve the system of overdetermined linear equations. Therefore, the least squares method can be used to solve overdetermined linear equations [20]. The least squares method is an optimization approach that uses the sum of squares of sample residuals as the loss function given a model. By setting the partial derivative to 0, it directly solves unconstrained optimization problems and obtains analytical solutions for the optimal model parameters. The least squares method can be used for curve fitting and can also express other optimization problems by minimizing energy or maximizing entropy. The least squares method is designed for the multivariate simple regression task of linear models, which requires labels to be 1-dimensional and the model to provide prediction results for sample feature vectors.

Therefore, the objective equation solved by the least squares method is set as:

$$M_{tar} = \sum_{x=1}^{n} \left(G_{ra}(x) - \eta \cdot N_{vec} \cdot L\right) \cdot \left(G_{ra}(x) - \eta \cdot N_{vec} \cdot L\right)^{T} \tag{10}$$

After the above process, the normal vector N_{vec} of the surface of the sphere can be obtained. However, in the process of collecting data, due to the splitting of reflected light on the surface of the object, the collected data information is discrete and local, resulting in the solved surface normal vector being also discrete and local. Therefore, after calculating the surface normal vector of the object, we further process it by separating, interpo-

lating, fitting, and merging the RGB images of the surface normal vector of the object. From the separated data in all directions and the surface normal vector diagram of the original object, it can be seen that due to the splitting of reflected light during data collection, the data is discrete and local, resulting in the solved surface normal vector being also discrete and local. In order to compensate for missing information, interpolation fitting estimation is performed on the calculated surface normal vectors of the object. Here, interpolation polynomials are used to fit the discrete values of the surface. This method can make the discrete data smooth and close to the true values after interpolation. The interpolation polynomial method is as follows:

Assuming the definition interval of the curve function is [m, n], where $x_{i,i\in[0,t]}$ represents t + 1 distinct points and each point corresponds to a value of $f(x_i)$, the interpolation polynomial is expressed as:

$$H_t(x)=\sum_{i=0}^{t}\alpha_i\cdot x^i \tag{11}$$

α_i is the interpolation coefficient. Organize the above formula into matrix form and express it as follows:

$$\begin{bmatrix}1 & x_0 & \cdots & x_0^{t-1} & x_0^t\\ 1 & x_1 & \cdots & x_1^{t-1} & x_1^t\\ \vdots & \vdots & \ddots & \vdots & \vdots\\ 1 & x_{t-1} & \cdots & x_{t-1}^{t-1} & x_{t-1}^t\\ 1 & x_t & \cdots & x_t^{t-1} & x_t^t\end{bmatrix}\begin{bmatrix}\alpha_0\\ \alpha_1\\ \vdots\\ \alpha_{t-1}\\ \alpha_t\end{bmatrix}=\begin{bmatrix}H_t(x_0)\\ H_t(x_1)\\ \vdots\\ H_t(x_{t-1})\\ H_t(x_t)\end{bmatrix} \tag{12}$$

The coefficient matrix is a Vandermonde matrix. According to the determinant property, the coefficient matrix is an t + 1-order Vandermonde determinant. Therefore, the equation has a unique solution.

4.3 Calculation of Surface Depth Information for Ship Curved Plates

The gradient field of the solved surface normal vector is calculated to obtain surface depth information. In this paper, the least squares method is used to estimate the depth information of the object surface. The principle of the least squares method is to find a surface function $C(x, y)$, which is the depth value of the object's surface, based on the relationship between the surface normal vector and the surface tangent plane [21]. Since the surface normal vector of an object is perpendicular to the tangent plane of the object surface, the surface normal vector is perpendicular to any straight line on the tangent plane; For any point (x_c, y_c) on the surface of an object, if the vectors pointing to the right, lower, left, and upper neighboring pixels are all located on the tangent plane passing through that point, then the vector pointing to the right neighboring pixel is:

$$\left(x_c+1,y_c,C_{x_c+1,y_c}\right)-\left(x_c,y_c,C_{x_c,y_c}\right)=\left(1,0,C_{x_c+1,y_c}-C_{x_c,y_c}\right) \tag{13}$$

If the pixel vector pointing to the right neighborhood of the point is perpendicular to the surface normal vector of the point, then the vertical equation is:

$$\left(1,0,C_{x_c+1,y_c}-C_{x_c,y_c}\right)\cdot N_{x_c,y_c}=0 \tag{14}$$

The normal vector of each point is perpendicular to the pixel vectors of the upper, lower, left, and right neighborhoods of that point. Therefore, four linear equation systems can be established about that point (excluding the topmost, bottommost, leftmost, and rightmost pixel points. Among them, the four vertices only have two linear equation systems for their neighborhoods, while the rest have three linear equation systems for their neighborhoods). Assuming the image size is H×W, the four neighborhood overdetermined linear equation system can be established through the above process to obtain the depth information of the surface.

5 Measurement Experiment and Result Analysis

Set up the experimental environment, and the main parameters of the computer in the experimental environment are shown in Table 5.

Table 5. Experimental environment and its parameters

Parameter	Parameter values
Size of collected images	2560*1920
The actual size of the input image	512*384
CPU	Inntel i7
Graphics card	RTX4070
Operating system	Ubuntu 23.04
Programming software	Pycharm
Programming Language	Python 3.6
Image processing library	opencv

Meanwhile, the measurement system was developed using C #, and the structure of the measurement system developed in this article is shown in Fig. 5.

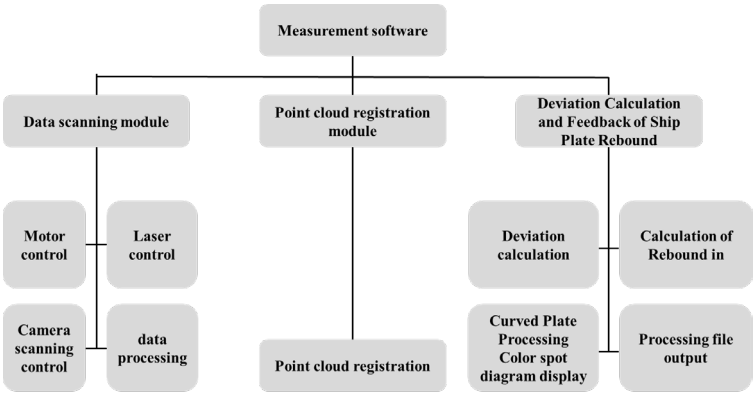

Fig. 5. Structure of detection system

The main page of the detection system is shown in Fig. 6.

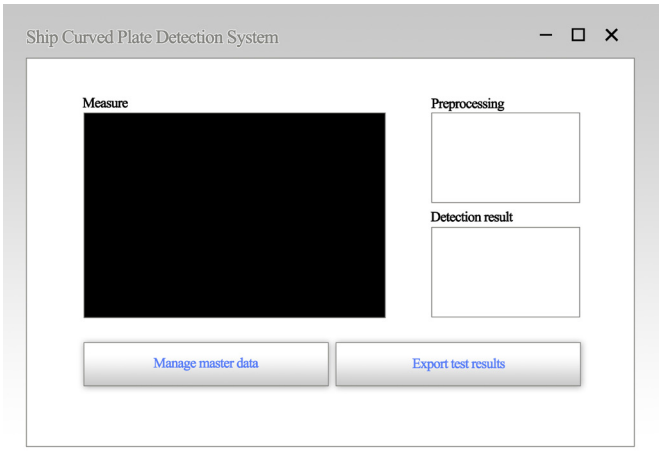

Fig. 6. System interface

During the test, place the measured object on the transmission platform of the image acquisition system and fix it to prevent the measured object from shaking due to inertia during the rotation process, resulting in rotation error. Then adjust the rotation platform angle to collect image data after each rotation, and collect 3, 6, 12 18. 24, 30, and 36 types of image data with multiple angles and different directions of rotating light sources (among which 6 types of image data with different directions of rotating light sources are obtained by adding 3 types of image data with different directions of rotating light sources on the premise of the first 3 types of image data with different directions of rotating light sources, for a total of 6 types of image data with different directions of rotating light sources; 12 types are obtained by adding 6 types of image data with different directions of rotating light sources on the premise of the first 6 types of image data with different directions of rotating light sources, for a total of 12 types of image data with different directions of rotating light sources, and so on, until 36 types of image data with different directions of rotating light sources are obtained. Firstly, the collected image data is pre-processed to remove unnecessary noise and estimate the direction of light sources in the deno; Secondly, based on the estimated light source direction, object surface normal vector, and the relationship between image pixel intensity, the object surface normal vector is jointly solved, and then the object surface normal vector is interpolated and fitted to compensate for the lack of data information; Again, based on the principle that the normal vector of the object surface is perpendicular to the tangent plane of the object surface, solve for the depth information of the object surface; Finally, the obtained depth information is used to restore the curvature of the object and detect errors.

The test object is shown in Fig. 7.

Fig. 7. Curved parts

The measurement results are shown in Fig. 8 and Fig. 9.

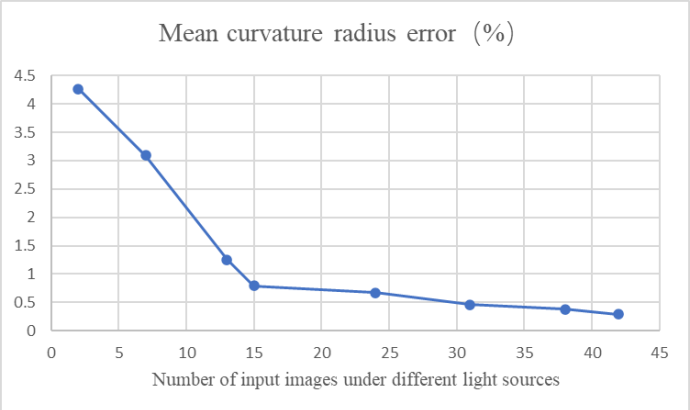

Fig. 8. Mean error of curvature radius

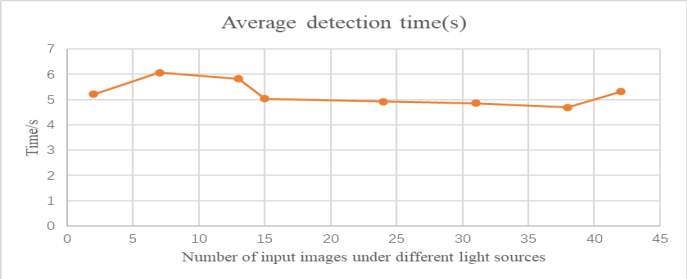

Fig. 9. Detect average running time

The average error and average running time of the object surface restoration results obtained from image data collected at 2, 7, 13, 15, 24, 31, 38, and 42 different angles and directions of rotating light sources are shown in Fig. 8 and Fig. 9. From the figure, it can be seen that as the number of images under different light source directions increases, the two-dimensional images contain more and more three-dimensional information about the surface of the object. The increase in the amount of surface information of the object leads to higher accuracy in solving and restoring until it gradually stabilizes. At the same time, the increase in images leads to a slight increase in average running time, which is not particularly significant. However, the increase in the number of images during the acquisition process will significantly increase the acquisition time. In order to ensure the real-time and accurate detection efficiency, it is necessary to select an appropriate number of images for detection. According to the average error and running time in Fig. 8 and Fig. 9, it can be seen that the curvature radius error of 13 different rotating light source directions is 0.79%, and the curvature radius error of 38 different rotating light source directions is 0.38%, which is 0.41% lower than that of 13; The curvature radius error under 24 different rotating light source directions is 0.67%, which is a decrease of 0.12% compared to 185, but the decrease is not significant. It can be observed that as the number of images in different light source directions increases, the decrease in error gradually stabilizes. Although the increase in running time is not significant, the time taken to capture each image in different light source directions does not exceed 10 seconds. The increase in images gradually stabilizes the reduction in error rate, but leads to a significant increase in total time (acquisition time+running time). Therefore, the number of images cannot increase infinitely, and an appropriate number of images needs to be selected.

6 Conclusion

This article focuses on the demand for curvature detection of ship curved plates, and studies binocular vision detection technology. Drawing on the principles of manual sample detection using triangular templates and flexible splines, a ship curved plate system based on 3D vision measurement technology is developed to replace the traditional wooden triangular template detection method and flexible template detection method. The main research content and achievements of this article are as follows:

1) A binocular vision detection system has been established, and the selection of cameras and lenses has been completed. Domestic equipment has been selected for the camera selection, which has lower maintenance and usage costs. At the same time, domestic lenses have also been selected for the lenses. The selection of other equipment is not described in detail as it is a non core device;

2) The camera was calibrated using matrix transformation and other methods, and then the camera visual distortion was corrected. The correction results were verified through a checkerboard pattern;

3) We established equations for ship curvature and depth information, and then solved each equation using the least squares method. The process of solving is the calculation process;

4) Built a simulation experimental environment and conducted experimental measurements.

Meanwhile, based on practical experience, this article has some shortcomings on the basis of existing research results. In addition, with some of my recent research ideas, further research directions have been organized:

1) The equipment is lightweight and portable. At present, operators manually adjust the processing parameters of the curved plate bending forming equipment based on the deviation values detected, and carry out further

processing. Further research is needed on how to automatically adjust the processing parameters of the bending equipment based on the deviation values feedback from the portable detection system, generate new processing files, and reprocess.

2) In addition, further research is needed on how to collect, summarize, and analyze data during the ship's curved plate processing, establish a processing technology database, and achieve parameter prediction for curved plate processing in order to better guide the detection results of portable detection systems for curved plate processing.

3) Combining the ideas of artificial intelligence, an adjustment plan is proposed for measuring and evaluating curvature, and the processing method is intelligently adjusted to guide the improvement of curved plate processing accuracy.

7 Acknowledgement

Science and Technology Research Project of Colleges and Universities of Hebei Province Youth Fund Project —"Research on the Precision Detection Technology of Portable Ship Plate Rib Position Line Based on Machine Vision", Project Number: QN2024132.

References

[1] C.-M. Xu, Exploration of the Application of Intelligent Manufacturing Technology in the Shipbuilding Industry, Science & Technology Information (6)(2023) 15-18. DOI: 10.16661/j.cnki.1672-3791.2208-5042-3017

[2] S. Wang, Y.-B. Wang, J. Wang, R. Li, Development and Application of Line Heating Forming Difficulty Evaluation System for Curved Hull Plate, Ship Engineering 45(7)(2023) 143-147.

[3] H.-L. Fan, Y.-P. Liu, G. Qin, Curved Plate Inspection Technology Based on Digital Measurement, Naval Architecture and Ocean Engineering (4)(2020) 39-43.

[4] Z.-J. Wang, J.-B. Jing, S.-Y. Wang, Measurement method of vehicle outline size based on binocular vision, Electronic Measurement Technology (12)(2023) 150-156.

[5] J.-W. Zhang, H.-R. Li, T.-H. Luo, L.-S. Zhang, Research on the external size measurement for industrial pipes using multi-group binocular vision system, Electronic Measurement Technology 46(6)(2023) 137-146.

[6] X.-Y. Yan, F.-F. Lu, L.-S. Ge, Application Research of Improved AD-Census Transform in Binocular Ranging, Software Guide 21(8)(2022) 138-143.

[7] L. Zhao, Y. Yu, F. Yu, Y. Hu, Binocular Vision Measurement Method of Curved Hull Plate, Marine Technology 49(02) (2021) 50-55.

[8] S.-S. Zhao, Z.-F. Guo, P. Li, X. Wang, H. X. Liu, Y.-C. Zhu, Development of Onsite Detection and Automatic Shape Adjustment System for Formed Hull Plates Based on Line Laser Multi-camer Stereovision, Tool Engineering (6)(2023) 72-76.

[9] D.-L. Hu, Y. Hu, Y. Yu, P.-P. He, F. Yu, Research on Photogrammetric Method of Large size Curved Hull Plate, Journal of Wuhan University of Technology (Transportation Science & Engineering) (4)(2022) 638-643.

[10] J.-C. Wang, Y.-J. Xie R.-C. Yang, J.-C. Liu, H. Zhou, Numerical Analysis and Process Planning of Cold Bending and Press Forming of Curved Plate for Offshore Platform, Ship Engineering 43(4)(2021) 94-101.

[11] H.Y. Zhang, X.-Q. Jiao, X.-Z. Jia, Design of Binocular Vision Acquisition and Processing System, Fire Control & Command Control 48(7)(2023) 163-169.

[12] H.-R. Zhang, J. Zhou, B, Liu, H.-B. Wan, S.-C. Zhai, A System Calibration Method of Industrial Camera Based on Least Square Method, Computer & Digital Engineering 51(11)(2023) 2518-2523.

[13] Y.-L. Hou, X.-Y. Su, W.-J. Chen, Calibration Method of Distance Between Optical Center of Camera and Rotation Axis in Rotating Vision Measurement System, Acta Optica Sinica 42(21)(2022) 69-79.

[14] L.-H. Wang, L.-L. Li, H.-L. Guo, A Target-based Calibration Method, Beijing Surveying and Mapping 35(3)(2021) 372-375.

[15] Y.-D. Liu, Z.-T. Jia, Improved Calibration Method of Camera Internal Parameters Based on Nonlinear Optimization, Laser & Optoelectronics Progress 59(18)(2022) 347-355.

[16] J. Huang, S.-Y. Li, X.-H. Zhang, J.-M. Wu, High-precision Calibration Method of Binocular Camera Based on Halcon Calibration Target, Computer & Digital Engineering 50(4)(2022) 762-766.

[17] J.-Y. Li, B. Guo, W.-S. Jiang, Z. Luo, Distortion Correction of Manipulator Vision System Based on Collinearity, Modular Machine Tool & Automatic Manufacturing Technique (12)(2020) 121-124.

[18] L. Xiao, Improved image preprocessing algorithm based on median filter, Journal of Science of Teachers' College and University 43(10)(2023) 41-44.

[19] M.-Y. Ren, L.-Z. Wang, J.-B. Zhao, Z.-Z. Tang, Viewpoint planning of surface structured light scanning for complex surface parts, Chinese Optics 16(1)(2023) 113-126.
[20] H.-X. Sun, J.-X. Luo, Z.-S. Pan, Y.-Y. Zhang, Y.-J. Zheng, A Method for Solving Homography Matrix Based on Constrained Total east Squares, Computer Technology and Development 32(12)(2022) 50-56.
[21] X.-F. Li, Design of furniture freeform surface modeling scanning system based on multiple Kinect, Modern Electronics Technique 43(2)(2020) 154-156.